

2014

BioTechnology

An Indian Journal

FULL PAPER

BTAIJ, 10(20), 2014 [12007-12014]

Distance compensation for infrared sensors used for total temperature measurements of large area canopy

Tianhua Chen^{1*}, Chong Jin^{1,2}, Daming Dong²¹School of Computer and Information Engineering, Beijing Technology and Business University, Beijing 100048, (CHINA)²National Engineering Research Center for Information Technology in Agriculture, Beijing Academy of Agriculture and Forestry Sciences, Beijing 100097, (CHINA)

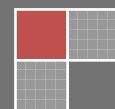
E-mail : cth188@sina.com

ABSTRACT

Measuring the total temperature of large area crop canopy is of great significance for grasping crop growth conditions. However, it is difficult to realize real-time measurements of the total temperature of large area canopy with traditional methods. The previously developed sensor based on the infrared detection technique for canopy temperature measurements achieved a large field of view (FOV) of 53.2° through the designed infrared optical system. The developed sensor allows the no-contact measurement of the total temperature of large area canopy. However, due to the influence of atmospheric transmission efficiency, the output data of the sensor are affected by the measurement distance. In this paper, we analyzed the influencing mechanism of the measurement distance on the measurement results and provided the distance compensation model to eliminate the influences of the measurement distance. With the distance compensation model, the measurement errors caused by the measurement distance are reduced from 1.4 °C to 0.2 °C. In addition, we added an ultrasonic module to the original sensor and designed a new type of sensor. After the verification through field experiments, the experiment results show that the advanced sensor can weaken the influence of the measurement distance effectively.

KEYWORDS

Canopy temperature; Infrared; Temperature measurements; Sensor; Distance compensation.



INTRODUCTION

Canopy temperature of crops is defined as the mean surface temperature of stems and leaves in different heights. At present, drought is the second most important influencing factor after plant diseases and pests^[1]. The increase of crop canopy temperature is caused by solar radiation absorption and the decrease is caused by transpiration. Canopy temperature is closely related to the water utilization status of crops, and the change of canopy temperature directly reflects the soil moisture distribution requirements of crops. Therefore, comprehensive monitoring of canopy temperature is one of the most important methods to ensure and improve crop yield and quality. Many years ago, Tanner proposed that canopy temperature was a valuable index to reflect the plant water utilization status. Zhang et al. investigated the canopy temperature of rice in the flowering stage and found that the canopy temperature increased with the decrease of the soil water content when the canopy temperature is lower than the air temperature^[2]. Grima et al. used canopy temperature to predict the grain yield of winter wheat^[3]. Chauhan et al. studied the influence of soil water distribution on the physiological parameters and grain yield during the reproductive stage of upland rice and found the canopy temperature was correlated to crop yield^[4]. Reynolds et al. demonstrated that measuring canopy temperature using infrared thermometry could increase the probability of identifying superior lines for improving the yield^[5]. Cai et al. studied the changing law of cotton canopy temperature and obtained the conclusion that canopy temperature increased with the increase of net radiation and air temperature and decreased with the increase of air saturation. Allen noted that the enhancement of photosynthesis and the decrease of transpiration rate would lead to the increase of canopy temperature under the condition of double CO₂ concentration^[6]. Therefore, the accurate measurement of the total temperature of crop canopy is of great significance.

Infrared thermometry can be used to detect the increase of canopy temperature caused by drought-induced stomatal closure. The detection results are helpful for irrigation decision and prediction of yield production. Leinonen et al. proposed a new method based on the thermal imaging technique and quantified the relationship between the change of canopy temperature and stomatal conductance by the fusion technology of thermal images and visible images^[7]. To measure the temperature of large area canopy, we developed a specific infrared temperature sensor. This sensor has the advantages of low cost, high sensitivity, non-destruction and non-contact. At the same time, the sensor can be used to measure the total temperature of large area crop canopy through the design of optical system with large field of view (FOV) and the specific setting of crop canopy emissivity. The distance coefficient of the sensor was designed to be 1.0 (the ratio of the distance from the sensor to the crop canopy to the diameter of the circular measurement area), and it owns a large FOV of 53.2°^[8]. We also studied the effects of different measurement distances on temperature measurements, and experimentally found that the distance greatly affected the measurement accuracy when the measurement distance was more than 60 cm. This paper aims to determine the influence mechanism of measurement distance on the sensor, provide a compensation approach to weaken the influence of measurement distance, and develop a new sensor that can be used to monitor the total temperature of crop canopy and is less susceptible to the measurement distance.

MATERIALS AND METHODS

Theoretical analysis

In the measurement of real temperature of opaque objects, the infrared radiation of the object surface is described as^[9]:

$$L_{\lambda} = \varepsilon_{\lambda} L_{b\lambda}(T_o) + (1 - \alpha_{\lambda}) L_{b\lambda}(T_u) \quad (1)$$

where T_o is the temperature of object surface; T_u is the ambient temperature; ε_{λ} is the surface emissivity of the tested object; α_{λ} is the surface absorption of the tested object.

The object temperature is determined through receiving the infrared radiation of object surface^[10]. During temperature measurements, the effective radiation received the infrared detector includes the self-radiation of objects, ambient radiation reflected by the objects and atmospheric radiation^[11]. The equation of incoming radiation can be established as:

$$E_{\lambda} = A_0 d^{-2} [\tau_{a\lambda} \varepsilon_{\lambda} L_{b\lambda}(T_o) + \tau_{a\lambda} (1 - \alpha_{\lambda}) L_{b\lambda}(T_u) + \varepsilon_{a\lambda} L_{b\lambda}(T_a)] \quad (2)$$

where A_0 is the visual area of the object corresponding to the minimum space opening angle of the detector; d is the distance between the detector and the object; $A_0 d^{-2}$ is a constant generally; T_a is the atmosphere temperature; $\tau_{a\lambda}$ is the atmospheric transmittance; $\varepsilon_{a\lambda}$ is the emissivity of the atmosphere.

For the infrared detector is applied in the very narrow waveband of 8 to 14 μm, it can be considered that ϵ_λ , α_λ , $\tau_{a\lambda}$ and $\epsilon_{a\lambda}$ are independent of wavelength λ and that the incoming radiation of working waveband can be converted into the voltage signal by the infrared detector:

$$V_s = A_R A_0 d^{-2} \{ \tau_a [\epsilon \int_{\lambda_1}^{\lambda_2} R_\lambda L_{b\lambda}(T_o) d\lambda + (1 - \alpha) \int_{\lambda_1}^{\lambda_2} R_\lambda L_{b\lambda}(T_u) d\lambda] + \epsilon_a \int_{\lambda_1}^{\lambda_2} R_\lambda L_{b\lambda}(T_a) d\lambda \} \tag{3}$$

where A_R is the lens area of the detector; R_λ is the spectral responsivity of the detector. Let $K = A_R A_0 d^{-2}$ and $\int_{\lambda_1}^{\lambda_2} R_\lambda L_{b\lambda}(T) d\lambda = I_R(T)$, then Eq. (3) becomes:

$$V_s = K \{ \tau_a [\epsilon I_R(T_o) + (1 - \alpha) I_R(T_u)] + \epsilon_a I_R(T_a) \} \tag{4}$$

It is usually assumed that the radiation received by the detector is identical to the radiation from a blackbody. Therefore $T_o = T_r$ if the temperature of a blackbody is T_r . If the object is a blackbody, then $\epsilon = 1$. Let $\tau_a = 1$, Eq. (4) can be obtained as:

$$V_s = K I_R(T_r) \tag{5}$$

If the object is regarded as a gray body, then $\epsilon = 1$ and $\tau_a = 1$ according to Kirchoff's Law^[12]. Substituting Eq. (5) into Eq. (4) gives the basic equation of temperature measurement as:

$$I_R(T_r) = \tau_a [\epsilon I_R(T_o) + (1 - \epsilon) I_R(T_u)] + (1 - \tau_a) I_R(T_a) \tag{6}$$

According to Planck's Law:

$$I_R(T) = \int_{\lambda_1}^{\lambda_2} R_\lambda L_{b\lambda}(T) d\lambda = \int_{\lambda_1}^{\lambda_2} R_\lambda \frac{C_1}{\pi} \lambda^{-5} [\exp(\frac{C_2}{\lambda T}) - 1]^{-1} d\lambda \tag{7}$$

where $C_1 = 3.7418 \times 10^{-12} (w \bullet cm^2)$ and $C_2 = 1.4388 (cm \bullet k)$. For the infrared detector, the variation of $I(T)$ with the temperature can be obtained:

$$I_R(T) \approx CT^n \tag{8}$$

where $n=9.2554$ for 3~5 μm ; $n=3.9889$ for 8~14 μm. Substituting Eq. (8) into Eq. (6) gives the computational equation of surface temperature as:

$$T_o = \{ \frac{1}{\epsilon} [\frac{1}{\tau_a} T_r^n - (1 - \epsilon) T_u^n - (\frac{1}{\tau_a} - 1) T_a^n] \}^{\frac{1}{n}} \tag{9}$$

It is usually assumed that atmospheric temperature is equal to ambient temperature: $T_u = T_a$. Then Eq. (9) can be rewritten as:

$$T_o = \{ \frac{1}{\epsilon} [\frac{1}{\tau_a} T_r^n + (\epsilon - \frac{1}{\tau_a}) T_a^n] \}^{\frac{1}{n}} \tag{10}$$

Differentiating two sides of Eq. (10) gives Eq. (11) as:

$$\frac{dT_o}{T_o} = \frac{1}{n \epsilon T_o^n} \{ [\epsilon (T_a^n - T_o^n)] \frac{d\epsilon}{\epsilon} + [\epsilon (T_a^n - T_o^n)] \frac{dT_a}{T_a} + (\epsilon - \frac{1}{\tau_a}) n T_a^n \frac{dT_a}{T_a} + \frac{n}{\tau_a} T_r^n \frac{dT_r}{T_r} \} \tag{11}$$

Therefore, it is obvious that the accuracy of temperature measurement is influenced by emissivity, atmospheric transmittance and the atmosphere temperature. Chrzanowski found that the emissivity of tested objects and atmospheric transmittance also affected the accuracy of temperature measurement through analyzing the infrared system^[13]. Ribeiro et al. also reported that the emissivity of crop canopy was approximately a constant in the 8-14 μm atmospheric window^[14]. Therefore, the influence of the emissivity on temperature measurement accuracy could be negligible and we regard atmospheric transmittance as the primary factor of measurement errors of T_o .

The absorption and scattering effects of atmosphere lead to the attenuation of infrared radiation received by the detector^[15]. The degree of atmospheric absorption varies with the measurement distance. When the distance between the object and the detector is increased, the influence of atmospheric transmittance on the measurement results becomes greater. Chrzanowski et al. measured the temperature of the blackbody at 90 °C with 760BB infrared camera within the 0.5-20 m range at the temperature of 18 °C and found that the measurement errors increased with the increase of the measurement distance.

The attenuation caused by the absorption and scattering of atmosphere can be expressed by atmospheric transmittance as^[16]:

$$\tau = e^{[-\alpha(\sqrt{d_o} - \sqrt{d_{cal}}) - \beta(d_o - d_{cal})]} \quad (12)$$

where τ is the atmosphere transmittance; α, β are constants; d_o is the object-system distance; d_{cal} is the calibration distance. Obviously, the temperature measurement errors caused by atmospheric transmittance are mainly due to the measurement distance, so we believe that the measurement errors caused by the influence of the atmospheric transmittance are closely related to the object-system distance. Then we carried out the experiment of distance compensation for the infrared sensor to improve the measurement accuracy.

Experimental design of distance compensation

Experiment equipment is shown in Figure 1. An infrared temperature sensor with a large FOV of 53.2° was adopted^[8]. Because the distance coefficient of the sensor was set to be 1.0, we prepared a 25 cm high round rubber container with the diameter of 140 cm. The MS6252B digital anemometer made by MASTECH Company (Guang Dong, China) was used to measure ambient temperature. The mercury thermometer with the measurement range of 0-50°C meeting the Chinese National Standard was adopted. In addition, the sensor should always be perpendicular to the water level during temperature measurements. Therefore, the sensor and the mercury thermometer were hung on the three-cornered holder with the range scale that made by ourselves, which allows us to adjust the measurement distance exactly.

In the preparation stage, the experiment was conducted at the constant room temperature. We injected water into the container to the 10-cm height and covered the bottom of the container completely with water. Meanwhile we put the mercury thermometer into the water and kept it away from contacting with the container wall. Then we started the infrared sensor and began the measurement after the sensor and water temperature became steady.

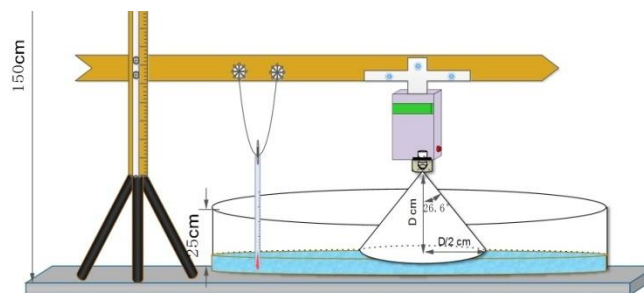


Figure 1 : The equipment of the experiment

In the measurement stage, in order to obtain the data under different ambient temperatures, the measurement was conducted at 9 a.m., 12 a.m., 15 p.m. and 19 p.m., respectively. In the experiment, we only considered the effect of the variation of measurement distance on the measurement results by the infrared sensor. We assumed that the ambient temperature and the water temperature were constant during the process of measurement and had no effect on the measured results. Firstly, we measured the ambient temperature and the water temperature with MS6252B digital anemometer and mercury thermometer simultaneously. Secondly, we placed the infrared sensor in the height 2.5 cm above the water level and recorded the measured results. Consequentially, the distance between the sensor and the water surface was changed from 2.5 to 100 cm according to the interval of 2.5 cm and the data of each measuring point were measured and recorded within 10 s.

At last, we repeated the measurements in four different periods to obtain the results measured under different ambient temperatures.

The design of new type of sensor

According to the experiment results and analysis data mentioned above, we observed that the change of distance led to the measurement errors of the infrared sensor with a large FOV. In order to avoid the disadvantage of the sensor and compensate for the measurement errors caused by the measurement distance, we developed the advanced infrared sensor with the function of distance compensation on the basis of the original sensor. The structure diagram of the new type of sensor is shown in Figure 2.

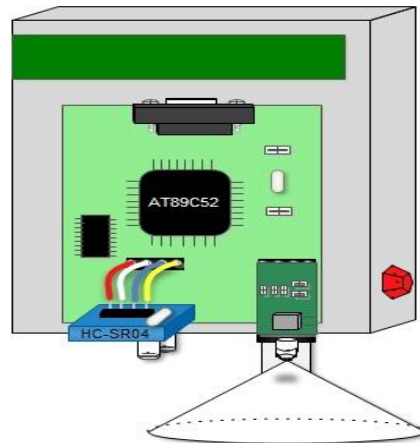


Figure 2 : The anatomy of the advanced infrared sensor

The HC-SR04 ultrasonic ranging module produced by JIE SHEN Co. Ltd. (Shen Zhen, China) is composed of the ultrasonic transmitter and acceptor. It can emit the 40 KHz square wave and detect the echo signal automatically. Furthermore, it can be valid for the measurement accuracy of 3mm within the range of 2 to 400 cm. And the effective voltage is 5V and the operating frequency is 40 KHz. The infrared temperature sensor containing the ultrasonic ranging module could measure the temperature and the distance between the detector and the tested object simultaneously. Therefore, the output data are defined as the sum of temperature measured by infrared sensor and the compensated temperature. And this model run on the microcontroller can compensate for the measured results. Therefore, we enhance the temperature measurement accuracy of the infrared sensor with a large FOV and there are steady measured results over the entire distance range of 5-100 cm. The specific compensation model is described in detail in the following section of results and analysis.

Verification experiment of the new type of sensor

Here, the measurement method of crop canopy temperature with the advanced infrared temperature sensor in the field was consistent with the experimental method used by Wang et al.^[8]. During the experiment, the temperature of crop canopy was considered to be constant. We selected a large area of the crop canopy and placed the sensor above the canopy. Then we changed the measurement distance gradually in the distance range of interest and recorded each measured result.

RESULTS AND DISCUSSION

Influence of distance and the model of compensation

In the experiment results respectively measured at 9 a.m., 12a.m., 15p.m. and 19 p.m. During the measurement, the ambient temperature and the water temperature are constant and only the measurement distance is changed. As discussed in the section of theoretical analysis, this effect mainly results from the increase of atmospheric transmittance between the detector and the canopy with the increase of the measurement distance. Consequentially, the radiation energy received by the detector decreased. Because the experiment was conducted in four different ambient temperatures, in order to eliminate the impacts of different ambient temperatures, a unified variable ΔT (the measurement error is calculated as the difference between the temperature measured by the sensor and the real temperature obtained by the mercury thermometer) is used to establish the relationship with the measured distance.

As shown in Figure 3, a, b, c, and d are respectively the corresponding variation trend diagram of the measurement errors with the increase of measurement distance under different ambient temperatures. It can be seen that, the measurement errors increase gradually when the measurement distance is increased with the interval of 2.5cm. The variation trends of the measurement errors are almost the same under four different ambient temperatures.

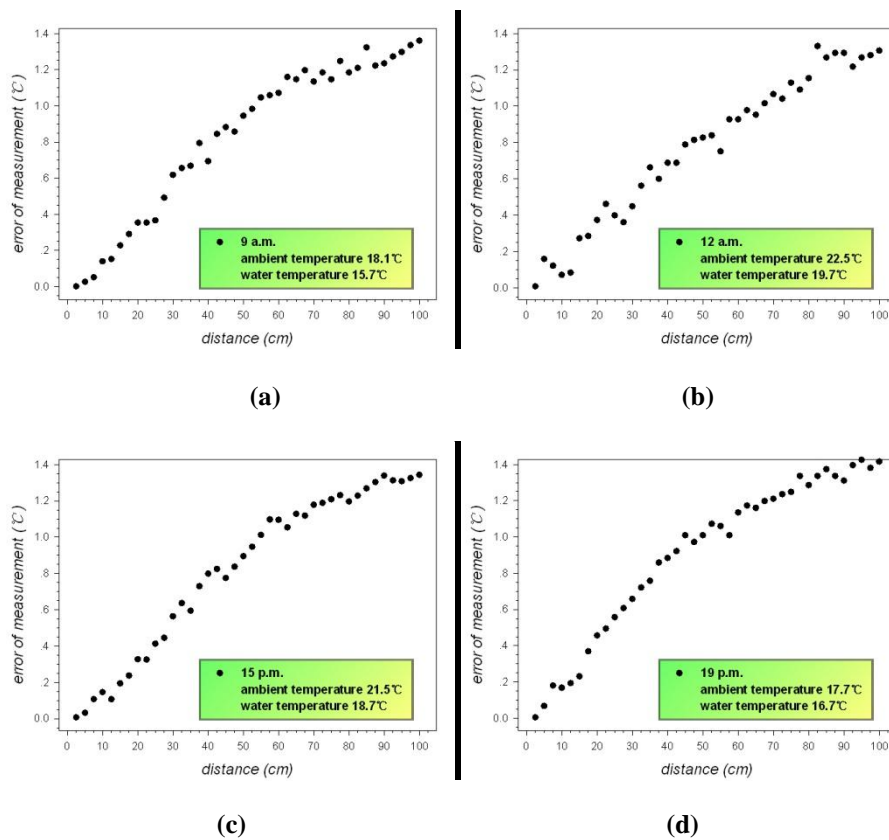


Figure 3 : The scatter diagram of distance-error: (a) variation trend of measured error with detection distance at 9a.m. (b) variation trend of measured errors with detection distance at 12a.m (c) variation trend of measured errors with detection distance at 15p.m (d) variation trend of measured errors with detection distance at 19p.m

In order to obtain the relationship between the measurement error (ΔT) and the measurement distance in the whole day and the distance-error fitting curve without the influence of ambient temperature, the temperature variation trends obtained under four different ambient temperatures are combined together to plot fitting curves. As shown in Figure 4, according to the distance-error curve, we can obtain the relationship between the measurement distance and measurement errors. And the equation of temperature compensation is expressed as:

$$y = -1.15 \times 10^{-4} \times \chi^2 + 0.026 \times \chi - 0.104 \quad (13)$$

where y is the value of temperature compensation (ΔT). Consequentially, the corresponding compensated value can be calculated for the different measurement distances according to Eq. (13). In this way, the influence of the variation of measurement distance could be decreased and the measured results could be relatively steady in the distance of 2.5-100 cm.

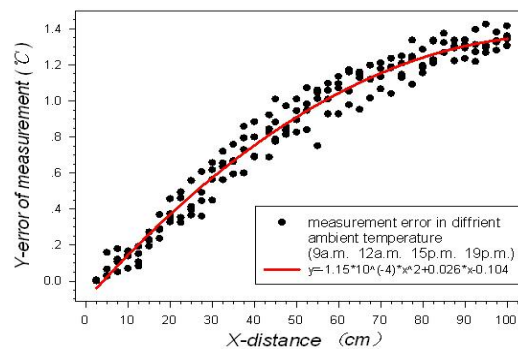


Figure 4 : The fitting curve of distance-error

According to the comparison of pre-compensation and post-compensation results obtained through the distance-error equation under the four different ambient temperatures (Figure 5), the measurement errors without the correction are between 1.2 and 1.4 °C. Wang et al. obtained the similar conclusion in the study on canopy temperature, but the impact of

distance turned out to be insignificant in the distance of 5-60 cm. This phenomenon may be interpreted as follows: their experiment is carried out in the field and the temperature of canopy may be changed during temperature measurement. As shown in Figure 5, the model of temperature compensation can work well under the four different ambient temperatures. The measured results after compensation are relatively steady and the measurement errors are controlled within the range of -0.2 to +0.2°C in the entire measurement distance. It is obvious that the effect of the measurement distance on the infrared sensor can be weakened to a large extent and that the precision and stability of the infrared temperature sensor can be improved. In addition, the temperature measurement model is inserted into the new type of sensor with the ultrasonic ranging module.

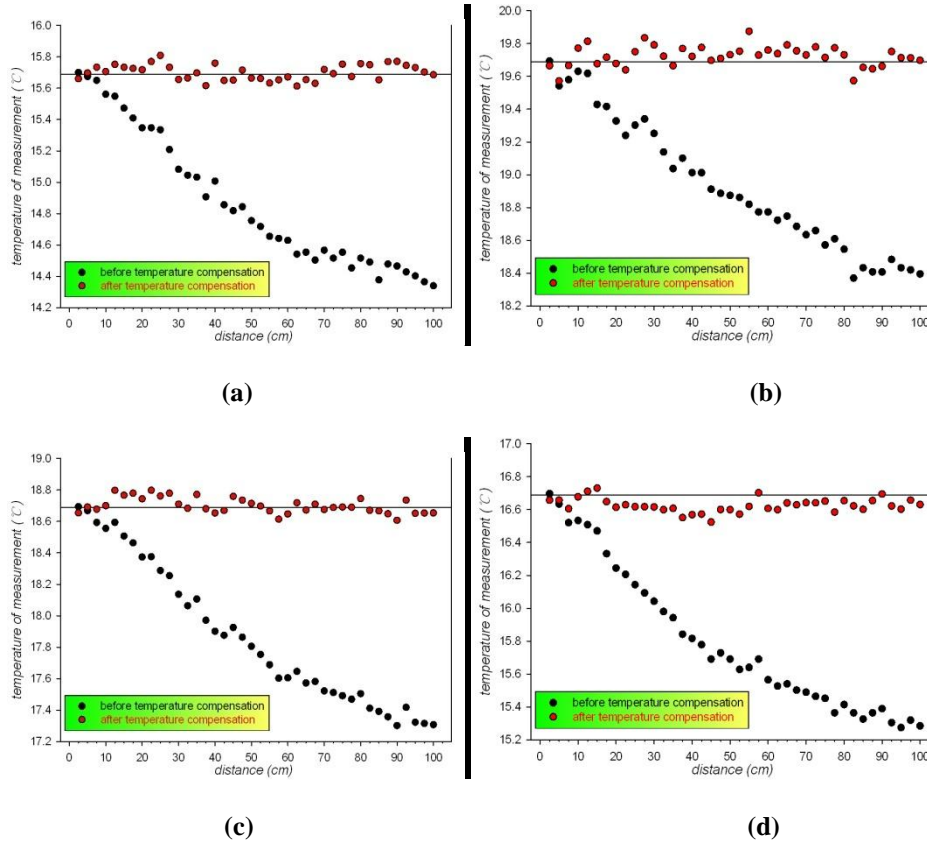


Figure 5 : Comparison of the measuring results before and after distance compensation. (a) 9a.m, (b) 12a.m, (c) 15p.m, (d) 19p.m.

Analysis of verification experiment results

In the experiment, we placed the advanced sensor above the large area crop canopy to measure the canopy temperature directly. The results of the experiment can be seen clearly in Fig. 6, which demonstrate that the temperatures measured by a large-FOV infrared sensor with temperature compensation function does not decrease with the increasing measurement distance. It is also found that the measurement errors of each measurement distance are below 0.2°C, indicating that the method can decrease the distance effect. As presented in Figure 6, the measurement temperatures change greatly within the distance less than 55 cm. For the measurement area is smaller when the measurement distance is smaller, the air flow leads to the variation of local temperature. However, the variation of local temperature accounts for a lower share of the average temperature variation when the measurement distance is long.

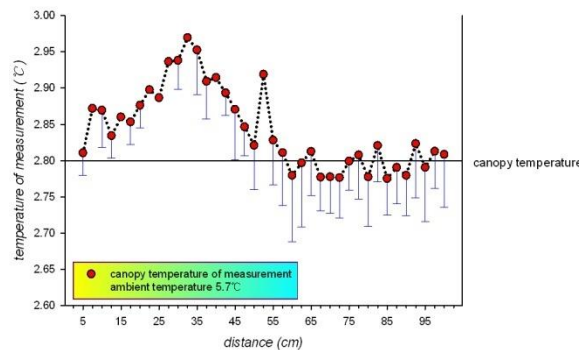


Figure 6: Measuring results of the new sensor at different distances

CONCLUSIONS

According to the fact that the measurement errors of infrared sensor with a large FOV can be caused by the measurement distance easily, in the paper, the distance compensation for the infrared sensor can be used to measure large-area crop canopy temperature. This work provides an effective compensation method on the basis of the effect of measurement distance and designs a new type of infrared sensor. Through the experiment and analysis, we reached a conclusion that when the detection distance increases, the measurement errors become larger and larger. We further formulated a distance–error equation, which is integrated into the new type of sensor. Then the advanced sensor is adopted in the measurement of canopy temperature in the field and the results show that the data obtained from the new sensor are controlled within the range of -0.2 to $+0.2^{\circ}\text{C}$.

REFERENCES

- [1] D.G.Dong; Relationship between canopy temperature and soil moisture. *Chinese Science Bulletin*, **31(8)**, 608-608 (1986).
- [2] W.Z.Zhang, Y.D.Han, H.J.Du; Relationship between canopy temperature at flowering stage and soil water content, yield components in rice. *Rice Science*, **14(1)**, 67-70 (2007).
- [3] K.Girma, K.L.Martin, R.H.Anderson, et al; Mid-season prediction of wheat-grain yield potential using plant, soil, and sensor measurements. *Journal of Plant Nutrition*, **29(5)**, 873-897 (2006).
- [4] J.S.Chauhan, T.B.Moya, R.K.Singh, et al; Influence of soil moisture stress during reproductive stage on physiological parameters and grain yield in upland rice. *Oryza*, **36(2)**, 130-135 (1999).
- [5] M.P.Reynolds, S.Rajaram, K.D.Sayre; Physiological and genetic changes of irrigated wheat in the post–green revolution period and approaches for meeting projected global demand. *Crop Science*, **39(6)**, 1611-1621 (1999).
- [6] L.H.Allen; Plant responses to rising carbon dioxide and potential interactions with air pollutants. *Journal of Environmental Quality*, **19(1)**, 15-34 (1990).
- [7] I.Leinonen, H.G.Jones; Combining thermal and visible imagery for estimating canopy temperature and identifying plant stress. *Journal of Experimental Botany*, **55(401)**, 1423-1431 (2004).
- [8] M.Wang, D.Dong, W.Zheng, et al; Using Infrared Sensor for Large Area Canopy Total Temperature Measurements of Rice Plants. *Applied Engineering in Agriculture*, **29(1)**, 115-122 (2013).
- [9] S.A.O'Shaughnessy, M.A.Hebel, S.R.Evett, et al; Evaluation of a wireless infrared thermometer with a narrow field of view. *Computers and Electronics in Agriculture*, **76(1)**, 59-68 (2011).
- [10] T.Hamrelius; Accurate temperature measurement in thermography, *Quantitative Infrared Thermography Conference*. 94 (1997).
- [11] T.Hamrelius; Accurate temperature measurement in thermography: an overview of relevant features, parameters, and definitions, Orlando'91, Orlando, FL. *International Society for Optics and Photonics*, 448-457 (1991).
- [12] K.Chrzanowski; Non-contact thermometry: measurement errors. *SPIE Polish Chapter*, (2001).
- [13] K.Chrzanowski; Influence of measurement conditions and system parameters on accuracy of remote temperature measurement with dualspectral IR systems. *Infrared physics & technology*, **37(3)**, 295-306 (1996).
- [14] B.Ribeiro da Luz, J.K.Crowley; Spectral reflectance and emissivity features of broad leaf plants: Prospects for remote sensing in the thermal infrared (8.0–14.0 μm). *Remote sensing of environment*, **109(4)**, 393-405 (2007).
- [15] A.Rogalski, K.Chrzanowski; Infrared devices and techniques. *Optoelectronics Review*, **2**, 111-136 (2002).
- [16] S.Pokorni; Error analysis of surface temperature measurement by infrared sensor. *International journal of infrared and millimeter waves*, **25(10)**, 1523-1533 (2004).